

Explicit Ensemble Mean Clock Synchronization for Optimal Atomic Time Scale Generation

Takayuki Ishizaki¹, Takahiro Kawaguchi², Yuichiro Yano³, Yuko Hanado³

Abstract—This paper presents a novel theoretical framework for atomic time scale generation, called explicit ensemble mean synchronization, which unifies clock synchronization and time scale generation within a control-theoretic paradigm. By exploiting an observable canonical decomposition of a standard atomic clock ensemble model, the system is decomposed into two complementary components: the observable part, which represents the synchronization deviation, and the unobservable part, which captures the synchronization destination. Within this structure, we mathematically prove that standard Kalman filtering, widely used in current time scale generation, can be interpreted as a special case of the proposed framework that optimizes long-term frequency stability in terms of the Allan variance. Furthermore, by applying appropriate state feedback control to each component based on the Kalman filtering, both clock synchronization and optimal time scale generation are achieved within a unified framework. This framework provides a principled basis for robust timekeeping systems that goes beyond conventional approaches in both scope and performance.

Keywords—Time scale generation, atomic clock synchronization, Kalman filtering, explicit ensemble mean.



1 INTRODUCTION

1.1 Background

Time scale generation from an ensemble of atomic clocks has long been a cornerstone technique in time and frequency metrology, particularly in the construction of national and international time references such as Coordinated Universal Time (UTC) [1]–[3]. In addition, this approach plays a critical role in the realization of resilient timing infrastructures that operate robustly even in the absence of reference time derived from, e.g., Global Navigation Satellite System (GNSS) signals, as exemplified by the concepts of composite clocks and the continuously operating primary reference time clock, the Coherent Network Primary Reference Time Clock (cn-PRTC) [4], [5].

In practice, a time scale, or standard time reference, is generated and maintained by regulating the frequency of local oscillators based on the ensemble time, i.e., the atomic time (TA) generated from multiple pairwise clock difference measurements [6]. While a number of studies have explored methods to compute the TA as a reference, these efforts have generally stopped short of addressing the integrated system design, including frequency regulation and steering of the actual oscillators. In particular, a unified theoretical framework based on systems and control theory that systematically addresses clock synchronization and time scale generation has not been thoroughly established. Furthermore, little attention has been paid to mathematically proving the underlying stability and convergence properties of such an integrated system, issues that are critical to both short-term and long-term reliability of resilient timekeeping infrastructures.

Kalman filtering has been widely used in this context [7] due to its ability to provide optimal state estimation under Gaussian noise assumptions. It has been used to derive the ensemble time by implicitly computing a synchronized mean of the clock states, called the implicit ensemble mean. However, it is well known that the Kalman filter algorithm suffers from certain limitations in this application. In particular, the error covariance matrix diverges over time, even though the Kalman gain converges to a constant value. This divergence implies the presence of indeterminate operations in the algorithm, which can lead to numerical instability. To address this issue, several error covariance reduction schemes have been proposed in the literature [8], [9].

Furthermore, it has been observed that optimal Kalman filtering, although statistically optimal in a general sense, often leads to suboptimal time scales in terms of short-term frequency stability. While an ad hoc method has been introduced to mitigate this problem [10], the underlying mechanism has not been theoretically elucidated.

1.2 Contributions

In this paper, we develop a unified and rigorous framework, referred to as “explicit ensemble mean synchronization,” that integrates time scale generation, ensemble clock synchronization, and oscillator control within a coherent systems and control theory paradigm. This framework provides an explicit understanding of how the standard Kalman filtering approach implicitly realizes ensemble mean time scales, referred to as implicit ensemble mean, and provides a systematic way to improve upon it. In particular, the main contributions of this paper are as follows.

- We derive an equivalent formulation of the Kalman filtering algorithm that completely eliminates indeterminate operations leading to the error covariance divergence by applying a specially tailored observ-

¹ Institute of Science Tokyo, 2-12-1, Ookayama, Meguro, Tokyo, 152-8552, Japan

² Gunma University, 1-5-1, Tenjincho, Kiryu, Gunma, 376-8515, Japan

³ National Institute of Information and Communications Technology, 4-2-1, Nukui-Kitamachi, Koganei, Tokyo, 184-8795, Japan

Manuscript received April 19, 2005; revised August 26, 2015.

able canonical decomposition to a standard atomic clock ensemble model.

- We construct a control algorithm that synchronizes all clocks in the ensemble to a free-running ensemble mean dynamics, the weighting of which can be explicitly specified by the user.
- We mathematically prove that conventional time scale generation using Kalman filtering is a special case of the proposed explicit ensemble mean synchronization, which achieves the least Allan variance only in the long term.
- We design a novel ensemble mean synchronization algorithm that explicitly balances both short-term and long-term frequency stability of the generated time scale by incorporating intermittent feedback control of the synchronization destination.

These contributions provide a rigorous foundation for resilient timekeeping infrastructures and open new avenues for optimizing atomic time scale generation through advanced control-theoretic techniques.

1.3 Mathematical Preliminaries

1.3.1 Symbols

Throughout the paper, we use the following symbols.

\mathbb{R}	the set of real numbers
\mathbb{Z}	the set of integers
$\mathbf{1}_N$	the N -dimensional all-ones vector
I_N	the N -dimensional identity matrix
A^\top	the transpose of a matrix A
$\text{im } A$	the image of a matrix A
$\text{ker } A$	the kernel of a matrix A
$\Lambda(A)$	the set of the eigenvalues of a square matrix A
$\mathbb{E}[X]$	the mean of a random variable X

Other symbols will be explained when used. We use the equality “:=” in the sense that a new symbol on the left is defined by known symbols on the right.

The Kronecker product of matrices is denoted by

$$A \otimes B := \begin{bmatrix} a_{11}B & \cdots & a_{1n}B \\ \vdots & \ddots & \vdots \\ a_{m1}B & \cdots & a_{mn}B \end{bmatrix}$$

where a_{ij} is the (i, j) -element of A . In this paper, we use the property of multiplication

$$(A \otimes B)(C \otimes D) = AC \otimes BD.$$

For a sequence $\{x[k]\}_{k \in \mathbb{Z}}$, the first-order difference operation is denoted by

$$\Delta_m x[k] := x[k+m] - x[k]$$

where m denotes an interval. In the same way, the second-order difference operation is denoted by

$$\Delta_m^2 x[k] := x[k+2m] - 2x[k+m] + x[k],$$

which is equal to $\Delta_m(\Delta_m x[k])$.

1.3.2 Gaussian Processes

A sequence $\{x[k]\}_{k \in \mathbb{Z}}$ of random variables is said to be a Gaussian process if the whole sequence follows a multivariate Gaussian distribution. Furthermore, a Gaussian process is said to be stationary if there exist some constant parameters μ and r_{ij} for $(i, j) \in \mathbb{Z}^2$ such that

$$\mathbb{E}[x[k]] = \mu, \quad \mathbb{E}[(x[k+i] - \mu)(x[k+j] - \mu)^\top] = r_{ij}$$

for any $k \in \mathbb{Z}$. In particular, it is said to be white if

$$\mu = 0, \quad r_{ij} = 0, \quad \forall i \neq j.$$

In this paper, the family of zero mean stationary Gaussian processes is denoted by \mathcal{G} .

Consider a discrete-time linear system

$$x[k+1] = Ax[k] + v[k]$$

driven by a white Gaussian process $\{v[k]\}_{k \in \mathbb{Z}}$. Clearly, the state sequence $\{x[k]\}_{k \in \mathbb{Z}}$ is a Gaussian process. In addition, the zero mean stationarity of the state process is equivalent to system stability in the sense that

$$\{x[k]\}_{k \in \mathbb{Z}} \in \mathcal{G} \iff \Lambda(A) \subseteq \mathbb{D}$$

where the unit disk in the complex plane is denoted by

$$\mathbb{D} := \{z \in \mathbb{C} : |z| < 1\}.$$

In such a way, the symbol \mathcal{G} will be used to represent the system stability, or the boundedness of the variance.

2 PROBLEM SETTING

2.1 Single Atomic Clock Model

2.1.1 Continuous-Time Model

In this paper, we discuss a standard second-order atomic clock model [7], [11], although similar analysis can be applied also to higher-order clock models. It is known from experimental observations that the time series of clock reading deviation relative to an ideal time coordinate can be mathematically modeled as a multiple integration of white Gaussian processes. In particular, the second-order model is given as

$$h(t) = c_1 + c_2 t + \int_0^t v_1(t_1) dt_1 + \int_0^t \int_0^{t_1} v_2(t_2) dt_2 dt_1 \quad (1)$$

where c_i is a scalar constant of the initial value, and

$$v_i = \{v_i(t) : t \in \mathbb{R}\}$$

denotes a continuous-time white Gaussian process such that

$$\begin{aligned} \mathbb{E}[v_i(t)] &= 0 \\ \mathbb{E}[v_i(t)v_i(t+\tau)] &= \sigma_i^2 \delta(\tau) \\ \mathbb{E}[v_1(t)v_2(t+\tau)] &= 0, \quad \forall \tau \in \mathbb{R}, \end{aligned} \quad (2)$$

where $\delta(\cdot)$ denotes the Dirac delta function. The integral equation model in (1) can be represented by a system of stochastic differential equations as

$$\begin{cases} \dot{x}_1(t) = x_2(t) + v_1(t) \\ \dot{x}_2(t) = v_2(t) + u(t), \end{cases} \quad (3)$$

where a control input u is introduced to discuss frequency regulation. If the initial values are given such that

$$x_1(0) = c_1, \quad x_2(0) = c_2,$$

and the control input is not applied, then the first state variable x_1 represents the clock reading deviation of the free-running clock as

$$x_1(t) = h(t), \quad \forall t \in \mathbb{R}.$$

Furthermore, consider the stacked vectors denoted by

$$x(t) := \begin{bmatrix} x_1(t) \\ x_2(t) \end{bmatrix}, \quad v(t) := \begin{bmatrix} v_1(t) \\ v_2(t) \end{bmatrix},$$

where the first elements are related to phase and the second elements to frequency. Then, we can write the stochastic differential equation system in (3) in the matrix form as

$$\begin{cases} \dot{x}(t) = A_c x(t) + B_c u(t) + v(t) \\ h(t) = C_c x(t) \end{cases} \quad (4)$$

where $A_c \in \mathbb{R}^{2 \times 2}$, $B_c \in \mathbb{R}^2$, and $C_c \in \mathbb{R}^{1 \times 2}$ are defined as

$$A_c := \begin{bmatrix} 0 & 1 \\ 0 & 0 \end{bmatrix}, \quad B_c := \begin{bmatrix} 0 \\ 1 \end{bmatrix}, \quad C_c := [1 \quad 0]. \quad (5)$$

The process noise v_c is a white Gaussian process such that

$$\mathbb{E}[v(t)] = 0, \quad \mathbb{E}[v(t)v^\top(t + \tau)] = Q_c \delta(\tau), \quad \forall t \in \mathbb{R}.$$

where the covariance matrix is diagonal and given as

$$Q_c := \begin{bmatrix} \sigma_1^2 & 0 \\ 0 & \sigma_2^2 \end{bmatrix}.$$

Note that σ_1 is the standard deviation of the white frequency noise, and σ_2 is that of the random walk frequency noise. This is known as a cesium-type atomic clock model.

2.1.2 Equivalent Discrete-Time Model

Consider a discrete-time sequence in an ideal time coordinate. The interval between two adjacent times is assumed to be constant, or equivalently

$$t_k := \tau k, \quad k \in \mathbb{Z} \quad (6)$$

where τ denotes a sampling interval. The relation between $x(t_k)$ and $x(t_{k+1})$ in (4) can be formally expressed as

$$x(t_{k+1}) = e^{A_c \tau} x(t_k) + \int_{t_k}^{t_{k+1}} e^{A_c(t_{k+1}-t)} (B_c u(t) + v(t)) dt.$$

Suppose that a zero-order hold input is applied, namely

$$u(t) = u[k], \quad \forall t \in [k\tau, (k+1)\tau).$$

Then, we can derive a discrete-time model that is equivalent to the continuous-time model in (4) over the discrete time sequence as

$$\begin{cases} x[k+1] = Ax[k] + Bu[k] + v[k] \\ h[k] = Cx[k] \end{cases} \quad (7)$$

where $A \in \mathbb{R}^{2 \times 2}$, $B \in \mathbb{R}^2$, and $C \in \mathbb{R}^{1 \times 2}$ are defined as

$$A := \begin{bmatrix} 1 & \tau \\ 0 & 1 \end{bmatrix}, \quad B := \begin{bmatrix} \tau \\ 1 \end{bmatrix}, \quad C := [1 \quad 0], \quad (8)$$

the discrete-time state and clock reading deviation as

$$x[k] := x(t_k), \quad h[k] := h(t_k).$$

Furthermore, the process noise $\{v[k]\}_{k \in \mathbb{Z}}$ is a white Gaussian process such that

$$\mathbb{E}[v[k]] = 0, \quad \mathbb{E}[v[k]v^\top[k]] = Q, \quad \forall k \in \mathbb{Z}$$

where the covariance matrix is given as

$$Q := \begin{bmatrix} \tau\sigma_1^2 + \frac{\tau^3}{3}\sigma_2^2 & \frac{\tau^2}{2}\sigma_2^2 \\ \frac{\tau^2}{2}\sigma_2^2 & \tau\sigma_2^2 \end{bmatrix}. \quad (9)$$

2.2 Atomic Clock Ensemble Model

Consider an ensemble of N clocks, each of which is written as the single clock model in (7). In the following, the state and process noise of the i th clock are denoted by

$$x_i[k] := \begin{bmatrix} x_{1i}[k] \\ x_{2i}[k] \end{bmatrix}, \quad v_i[k] := \begin{bmatrix} v_{1i}[k] \\ v_{2i}[k] \end{bmatrix}$$

where the first elements are related to the phase and the second elements to the frequency. With a slight abuse of notation, we use the same symbols as those for the single clock model to represent the stacked versions

$$x[k] := \begin{bmatrix} \text{col}(x_{1i}[k])_{i \in \mathbb{N}} \\ \text{col}(x_{2i}[k])_{i \in \mathbb{N}} \end{bmatrix}, \quad v[k] := \begin{bmatrix} \text{col}(v_{1i}[k])_{i \in \mathbb{N}} \\ \text{col}(v_{2i}[k])_{i \in \mathbb{N}} \end{bmatrix}$$

where \mathbb{N} denotes the label set of clocks, and $\text{col}(\cdot)$ denotes the stacked column vector. In the same way, we denote the control input to the i th clock by $u_i[k]$, the clock reading deviation of the i th clock by $h_i[k]$, and

$$u[k] := \text{col}(u_i[k])_{i \in \mathbb{N}}, \quad h[k] := \text{col}(h_i[k])_{i \in \mathbb{N}}.$$

Then, we have the model of the atomic clock ensemble as

$$\begin{cases} x[k+1] = (A \otimes I_N)x[k] + (B \otimes I_N)u[k] + v[k] \\ y[k] = (C \otimes V)x[k] + w[k] \\ h[k] = (C \otimes I_N)x[k] \end{cases} \quad (10)$$

where $V \in \mathbb{R}^{(N-1) \times N}$ denotes a matrix that represents pairs of clocks whose phase difference is being measured. For example, the choice of

$$V = [I_{N-1} \quad \mathbf{1}_{N-1}] \quad (11)$$

corresponds to the case where the phase differences of the N th clock and others are measured. Furthermore, the measurement noise $\{w[k]\}_{k \in \mathbb{Z}}$ is supposed to be a white Gaussian process such that

$$\mathbb{E}[w[k]] = 0, \quad \mathbb{E}[w[k]w^\top[k]] = \mathbf{R}, \quad \forall k \in \mathbb{Z},$$

where $\mathbf{R} \in \mathbb{R}^{(N-1) \times (N-1)}$ is a positive definite covariance matrix. Supposing that each atomic clock is independent of the others, we have the covariance matrix $\mathbf{Q} \in \mathbb{R}^{2N \times 2N}$ of the process noise as

$$\mathbf{Q} := \begin{bmatrix} \tau\Sigma_1 + \frac{\tau^3}{3}\Sigma_2 & \frac{\tau^2}{2}\Sigma_2 \\ \frac{\tau^2}{2}\Sigma_2 & \tau\Sigma_2 \end{bmatrix} \quad (12)$$

where $\Sigma_1 \in \mathbb{R}^{N \times N}$ and $\Sigma_2 \in \mathbb{R}^{N \times N}$ are defined as

$$\Sigma_1 := \text{diag}(\sigma_{11}^2, \dots, \sigma_{1N}^2), \quad \Sigma_2 := \text{diag}(\sigma_{21}^2, \dots, \sigma_{2N}^2).$$

Note that σ_{1i} and σ_{2i} denote the standard deviations of the white frequency noise and random walk frequency noise of the i th clock, respectively.

2.3 Kalman Filtering for Time Scale Generation

2.3.1 Kalman Filtering Algorithm

We consider state estimation of the clock ensemble model in (10) based on the Kalman filtering [12]. To simplify the notation, we denote the ensemble system matrices by

$$\mathbf{A} := A \otimes I_N, \quad \mathbf{B} := B \otimes I_N, \quad \mathbf{C} := C \otimes V.$$

In the following, the prior and posterior state estimates are, respectively, denoted by

$$\hat{x}^-[k] := \mathbb{E}[x[k]|Y[k-1]], \quad \hat{x}[k] := \mathbb{E}[x[k]|Y[k]],$$

where we consider the expectation of the state conditional on the past measurement information

$$Y[k] := \{y[k], y[k-1], \dots\}.$$

The corresponding error covariances are defined as

$$\begin{aligned} \mathbf{P}^-[k] &:= \mathbb{E}[(x[k] - \hat{x}^-[k])(x[k] - \hat{x}^-[k])^\top], \\ \mathbf{P}[k] &:= \mathbb{E}[(x[k] - \hat{x}[k])(x[k] - \hat{x}[k])^\top]. \end{aligned}$$

Then, the Kalman filtering algorithm is obtained as

$$\left\{ \begin{array}{l} \hat{x}^-[k] = \mathbf{A}\hat{x}[k-1] + \mathbf{B}u[k-1] \\ \mathbf{P}^-[k] = \mathbf{A}\mathbf{P}[k-1]\mathbf{A}^\top + \mathbf{Q} \\ \mathbf{H}[k] = \mathbf{P}^-[k]\mathbf{C}^\top(\mathbf{C}\mathbf{P}^-[k]\mathbf{C}^\top + \mathbf{R})^{-1} \\ \mathbf{P}[k] = (\mathbf{I}_{2N} - \mathbf{H}[k]\mathbf{C})\mathbf{P}^-[k] \\ \hat{x}[k] = \hat{x}^-[k] + \mathbf{H}[k](y[k] - \mathbf{C}\hat{x}^-[k]), \end{array} \right. \quad (13)$$

where $\mathbf{H}[k]$ is called the Kalman gain. This algorithm minimizes the variance of the state estimation error

$$\mathbb{E}[\|\mathbf{G}e[k]\|^2] = \text{trace}(\mathbf{G}\mathbf{P}[k]\mathbf{G}^\top)$$

for any matrix \mathbf{G} , where the state estimation error is

$$e[k] := x[k] - \hat{x}[k].$$

This is known as the optimality of conditional expectation.

2.3.2 Application to Time Scale Generation

For an observable system, the Kalman filtering algorithm produces the state estimate such that

$$\{e[k]\}_{k \in \mathbb{Z}} \in \mathcal{G}$$

in steady state, or more specifically

$$\lim_{k \rightarrow \infty} \mathbb{E}[e[k]] = 0, \quad \lim_{k \rightarrow \infty} \mathbf{P}[k] = \mathbf{P}^*,$$

where \mathbf{P}^* is a positive semidefinite matrix. However, this does not hold for the clock ensemble model in (10) because it is not observable. In particular, there is a nontrivial unobservable subspace

$$\bigcup_{\lambda \in \mathbb{C}} \ker \begin{bmatrix} \lambda \mathbf{I}_{2N} - \mathbf{A} \\ \mathbf{C} \end{bmatrix} = \text{im}(\mathbf{I}_2 \otimes \mathbf{1}_N). \quad (14)$$

In systems and control theory, the observability for linear systems can be defined as the condition that the initial state is uniquely identified by the measurement sequence, provided that the process noise and measurement noise are zero. Several equivalent definitions and conditions of the observability are known for linear systems [13].

Due to the unobservability, the state estimation error of the clock ensemble model diverges over time along the unobservable subspace. In other words, although the state estimation error diverges, its synchronization error disappears with time. Specifically, we have

$$\{(\mathbf{I}_2 \otimes V)e[k]\}_{k \in \mathbb{Z}} \in \mathcal{G}.$$

Because $V\mathbf{1}_N$ must be zero from definition, we see that

$$\ker(\mathbf{I}_2 \otimes V) = \text{im}(\mathbf{I}_2 \otimes \mathbf{1}_N).$$

This means that multiplying $e[k]$ by $(\mathbf{I}_2 \otimes V)$ eliminates the component of the synchronized estimation error associated with the unobservable subspace. Thus, stabilizing the state estimate $\hat{x}[k]$ by the control input $u[k]$ so that

$$\{\hat{x}[k]\}_{k \in \mathbb{Z}} \in \mathcal{G} \iff \{x[k] - e[k]\}_{k \in \mathbb{Z}} \in \mathcal{G},$$

we can realize the clock synchronization

$$\{(\mathbf{I}_2 \otimes V)x[k]\}_{k \in \mathbb{Z}} \in \mathcal{G}.$$

The statistical properties of the synchronization destination, such as the magnitude of the variance and the rate of divergence, are essentially comparable to those of the state estimation error. Note that the estimation error of average clock reading deviation

$$\varepsilon[k] := (\mathbf{C} \otimes \frac{1}{N}\mathbf{1}_N^\top)e[k],$$

called the ensemble atomic time, can be used as a reference time scale. In this sense, the analysis of the state estimation error is essential for time scale generation.

2.4 Problems to Discuss

2.4.1 The Allan Variance

Suppose that the control input $u[k]$ is zero for a single clock model in (7). The Allan variance [14] is defined by

$$\sigma_A^2(\tau) := \mathbb{E} \left[\frac{(\Delta_1^2 h[k])^2}{2\tau^2} \right]$$

where the clock model should be considered as an implicit function of the sampling interval τ . In fact, the Allan variance of the free-running clock model is a function only of τ , and it can be analytically found [15], [16] as

$$\sigma_A^2(\tau) = \frac{1}{\tau}\sigma_1^2 + \frac{\tau}{3}\sigma_2^2, \quad (15)$$

where σ_1 is the standard deviation of the white frequency noise, and σ_2 is that of the random walk frequency noise. In this paper, we call such an explicit representation the analytical Allan variance.

On the other hand, when the control input is applied, the Allan variance is generally not a function of τ alone, nor can it be expressed analytically. In such a case, a statistical estimator of the Allan variance is computed from a measured data set. Suppose that an output sequence

$$\{h[k]\}_{k \in \mathbb{T}} := \{h[0], h[1], \dots, h[T]\}$$

is measured over the sampling interval τ . Then, a statistical estimator of the Allan variance can be computed as

$$\hat{\sigma}_A^2(m; \{h[k]\}_{k \in \mathbb{T}}) := \frac{1}{T-2m} \sum_{k=0}^{T-2m-1} \frac{(\Delta_m^2 h[k])^2}{2(m\tau)^2}$$

TABLE 1
Standard deviations of white frequency noise and random walk frequency noise.

scale	1	2	3	4	5	6	7	8	9	10	
σ_1	10^{-9}	0.1700	0.0886	0.1221	0.1273	0.2185	0.1063	0.1805	0.2168	0.0930	0.1801
σ_2	10^{-12}	0.1507	0.0532	0.0167	0.0771	0.2940	0.0492	0.0407	0.0829	0.0520	0.0566

TABLE 2
Standard deviations of measurement noise.

scale	(1,10)	(2,10)	(3,10)	(4,10)	(5,10)	(6,10)	(7,10)	(8,10)	(9,10)
10^{-14}	0.4353	0.0759	0.4720	0.1166	0.4148	0.0885	0.0998	0.2453	0.0373

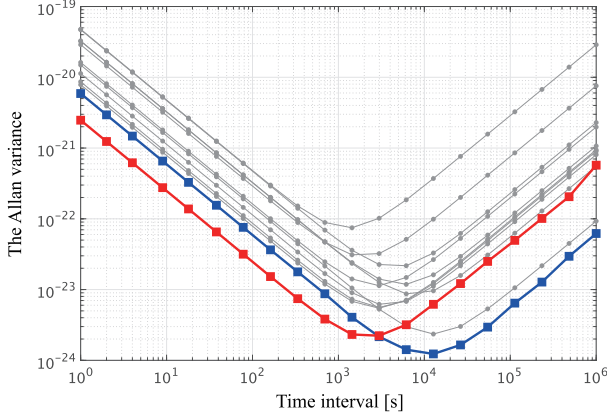


Fig. 1. The Allan variances. The black lines are the analytical Allan variance of the free-running clocks. The blue line is the statistical Allan variance of the reference time scale generated by the optimal Kalman filtering. The red line is the the statistical Allan variance of the reference time scale generated by the suboptimal Kalman filtering.

where m is an interval, and the set of feasible values is

$$\mathbb{M} := \{1, 2, \dots, \lfloor \frac{T-1}{2} \rfloor\}.$$

In this paper, we call this estimate the statistical Allan variance. Typically, the statistical Allan variance are presented as a double logarithmic plot of

$$\mathcal{L}\{h[k]\}_{k \in \mathbb{T}} := (\tau m, \hat{\sigma}_A^2(m; \{h[k]\}_{k \in \mathbb{T}}))_{m \in \mathbb{M}}.$$

This estimation is used as standard for the evaluation of generated time scales. In the following, for a vector-valued sequence $\{h[k]\}_{k \in \mathbb{T}}$, the operation \mathcal{L} should be understood in the element-wise sense.

2.4.2 Illustrative Problems

Consider an ensemble of 10 independent atomic clocks. The standard deviations of white frequency noise and random walk frequency noise are listed in Table 1, whose values are determined based on experiments. The standard deviations of measurement noise are listed in Table 2, where the phase differences are measured according to (11).

The analytical Allan variance in (15) is plotted by the black lines for each clock in Fig. 1. To this clock ensemble, we run the Kalman filtering algorithm in (13) to generate a reference time scale. Specifically, the Kalman filtering algorithm is calculated for the stochastic time evolution of the clock ensemble with the time length T of 10^7 [s] and

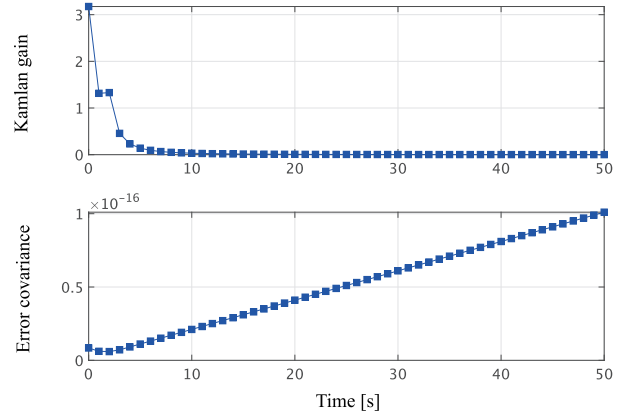


Fig. 2. Increments of the Kalman gain and error covariance. The upper subfigure shows the Frobenius norm of the increment of the Kalman gain. The lower subfigure shows that of the error covariance.

the sampling interval τ of 1 [s]. Then, the statistical Allan variance of the generated reference time scale $\mathcal{L}\{\varepsilon[k]\}_{k \in \mathbb{T}}$ is plotted by the blue line in Fig. 1. We can see that the statistical Allan variance of the reference time scale is better than the analytical Allan variance of each clock in both the short and long term.

As an illustration, using the same time series data, we show the result when the value of the noise covariance used in the Kalman filtering algorithm is artificially varied. In particular, in the recursion of (13), we use

$$\mathbf{Q} = \begin{bmatrix} (\tau \bar{\sigma}_1^2 + \frac{\tau^3}{3} \bar{\sigma}_2^2) I_{10} & \frac{\tau^2}{2} \bar{\sigma}_2^2 I_{10} \\ \frac{\tau^2}{2} \bar{\sigma}_2^2 I_{10} & \tau \bar{\sigma}_2^2 I_{10} \end{bmatrix}$$

where $\bar{\sigma}_i^2$ denotes the average of noise variances

$$\bar{\sigma}_i^2 := \frac{1}{10} \sum_{j=1}^{10} \sigma_{ij}^2.$$

Obviously, this setting is not optimal for the Kalman filtering because of the modeling error of the noise variances. The result is shown by the red line in Fig. 1. Interestingly, the result for this suboptimal case is better than that for the optimal case in terms of short term stability.

As shown above, optimal Kalman filtering is generally not optimal in terms of time scale generation. In addition to this problem, the Kalman filtering-based time scale generation also has the problem that the error covariance for calculating the Kalman gain diverges over time. This is

demonstrated in Fig. 2, where the Frobenius norms [17] of the increments, i.e., $\|\Delta_1 H[k]\|_F$ and $\|\Delta_1 P^-[k]\|_F$, are plotted. Note that even though the Kalman gain is calculated by the product of the error covariance and a constant matrix, it converges to a constant matrix over time. This implies that the Kalman filtering algorithm for clock ensembles contains ‘‘indeterminate’’ operations, such that a divergent value is annihilated by a matrix multiplication.

From these observations, we ask the following questions.

- Q1 Is it possible to find a Kalman filtering algorithm in a form that does not contain indeterminate operations?
- Q2 Is it possible to find a control algorithm that synchronizes all the clocks to a reference time scale?
- Q3 Is it possible to mathematically prove why the optimal Kalman filtering algorithm does not produce the optimal time scale?
- Q4 Is it possible to generate an optimal time scale based on the Kalman filtering algorithm that achieves both short-term and long-term frequency stability?

In this paper, we give clear solutions to all these questions in terms of systems and control theory. In particular, we develop a general framework, called explicit ensemble mean synchronization, that handles not only optimal time scale generation but also clock synchronization.

3 ANALYSIS OF KALMAN FILTERING ALGORITHM

3.1 All Observable Canonical Decompositions

We apply observable canonical decomposition [18] to the clock ensemble model in (10) for the analysis of the Kalman filtering algorithm in (13). For this purpose, we consider a basis expansion based on the unobservable subspace as

$$x[k] = \mathbf{W}((I_2 \otimes V)\mathbf{W})^{-1}\xi_o[k] + (I_2 \otimes \mathbf{1}_N)\xi_{\bar{o}}[k] \quad (16)$$

where $\mathbf{W} \in \mathbb{R}^{2N \times 2(N-1)}$ is a column full rank matrix that represents a parameter of the decomposition such that

$$\text{im } \mathbf{W} + \text{im}(I_2 \otimes \mathbf{1}_N) = \mathbb{R}^{2N}. \quad (17)$$

For the new state vector

$$\xi[k] := \begin{bmatrix} \xi_o[k] \\ \xi_{\bar{o}}[k] \end{bmatrix},$$

we have the one-to-one relationship as

$$\xi[k] = \mathbf{T}x[k] \iff x[k] = \mathbf{T}^{-1}\xi[k]$$

with the transformation matrices

$$\mathbf{T}^{-1} = \begin{bmatrix} \mathbf{W}((I_2 \otimes V)\mathbf{W})^{-1} & I_2 \otimes \mathbf{1}_N \\ & \end{bmatrix}, \quad (18)$$

$$\mathbf{T} = \begin{bmatrix} I_2 \otimes V \\ (\overline{\mathbf{W}}(I_2 \otimes \mathbf{1}_N))^{-1}\overline{\mathbf{W}} \end{bmatrix}$$

where $\overline{\mathbf{W}} \in \mathbb{R}^{2 \times 2N}$ is a row full rank matrix such that

$$\ker \overline{\mathbf{W}} = \text{im } \mathbf{W}. \quad (19)$$

This relationship implies that choosing the column space of \mathbf{W} is equivalent to choosing the row space of $\overline{\mathbf{W}}$. Note that $\xi_o[k]$ in (16) represents the unobservable state of the clock ensemble model because the unobservable subspace is given as in (14). On the other hand, $\xi[k]$ represents the observable state parameterized by \mathbf{W} .

Applying this basis expansion, or variable change, we have the new state-space realization as

$$\begin{cases} \xi[k+1] = \mathbf{T}\mathbf{A}\mathbf{T}^{-1}\xi[k] + \mathbf{T}\mathbf{B}u[k] + \mathbf{T}v[k] \\ y[k] = \mathbf{C}\mathbf{T}^{-1}\xi[k] + w[k]. \end{cases} \quad (20)$$

Note that the new system matrices have the structure of

$$\begin{aligned} \tilde{\mathbf{A}} &:= \mathbf{T}\mathbf{A}\mathbf{T}^{-1} = \begin{bmatrix} \mathbf{A}_o & 0 \\ \overline{\mathbf{U}}\mathbf{A}\mathbf{U} & \mathbf{A} \end{bmatrix}, \\ \tilde{\mathbf{B}} &:= \mathbf{T}\mathbf{B} = \begin{bmatrix} \mathbf{B}_o\mathbf{V} \\ \overline{\mathbf{U}}\mathbf{B} \end{bmatrix}, \\ \tilde{\mathbf{C}} &:= \mathbf{C}\mathbf{T}^{-1} = [\mathbf{C}_o \quad 0] \end{aligned}$$

where the generalized inverses are represented as

$$\mathbf{U} := \mathbf{W}((I_2 \otimes V)\mathbf{W})^{-1}, \quad \overline{\mathbf{U}} := (\overline{\mathbf{W}}(I_2 \otimes \mathbf{1}_N))^{-1}\overline{\mathbf{W}},$$

and the system matrices of the observable subsystem as

$$\mathbf{A}_o := \mathbf{A} \otimes I_{N-1}, \quad \mathbf{B}_o := \mathbf{B} \otimes I_{N-1}, \quad \mathbf{C}_o := \mathbf{C} \otimes I_{N-1}.$$

It is clear from the block triangular structure that the unobservable state $\xi_{\bar{o}}[k]$ has no effect on the output $y[k]$. This is a complete parameterization of the observable canonical decomposition of the clock ensemble model in (10).

3.2 Determinate Kalman Filtering Algorithm

Consider the Kalman filtering algorithm for the new state-space realization in (20) as

$$\begin{cases} \hat{\xi}^-[k] = \tilde{\mathbf{A}}\hat{\xi}^-[k-1] + \tilde{\mathbf{B}}u[k-1] \\ \tilde{\mathbf{P}}^-[k] = \tilde{\mathbf{A}}\tilde{\mathbf{P}}^-[k-1]\tilde{\mathbf{A}}^\top + \tilde{\mathbf{Q}} \\ \tilde{\mathbf{H}}[k] = \tilde{\mathbf{P}}^-[k]\tilde{\mathbf{C}}^\top(\tilde{\mathbf{C}}\tilde{\mathbf{P}}^-[k]\tilde{\mathbf{C}}^\top + \mathbf{R})^{-1} \\ \tilde{\mathbf{P}}[k] = (I_{2N} - \tilde{\mathbf{H}}[k]\tilde{\mathbf{C}})\tilde{\mathbf{P}}^-[k] \\ \hat{\xi}[k] = \hat{\xi}^-[k] + \tilde{\mathbf{H}}[k](y[k] - \tilde{\mathbf{C}}\hat{\xi}^-[k]) \end{cases} \quad (21)$$

where the symbols with the tilde are new variables. In fact, this Kalman filtering algorithm is equivalent to the original one in (13) because they have the one-to-one relationship as

$$\begin{aligned} \hat{\xi}^-[k] &= \mathbf{T}\hat{x}^-[k], \quad \hat{\xi}[k] = \mathbf{T}\hat{x}[k], \quad \tilde{\mathbf{H}}[k] = \mathbf{T}\mathbf{H}[k] \\ \tilde{\mathbf{P}}^-[k] &= \mathbf{T}\mathbf{P}^-[k]\mathbf{T}^\top, \quad \tilde{\mathbf{P}}[k] = \mathbf{T}\mathbf{P}[k]\mathbf{T}^\top, \quad \tilde{\mathbf{Q}} = \mathbf{T}\mathbf{Q}\mathbf{T}^\top. \end{aligned}$$

For the purposes of the following discussion, we denote the estimation error covariances by

$$\tilde{\mathbf{P}}^-[k] = \begin{bmatrix} \mathbf{P}_{oo}^-[k] & * \\ \mathbf{P}_{\bar{o}\bar{o}}^-[k] & \mathbf{P}_{\bar{o}\bar{o}}^-[k] \end{bmatrix}, \quad \tilde{\mathbf{P}}[k] = \begin{bmatrix} \mathbf{P}_{oo}[k] & * \\ \mathbf{P}_{\bar{o}\bar{o}}[k] & \mathbf{P}_{\bar{o}\bar{o}}[k] \end{bmatrix},$$

where the symmetric parts are omitted. Note that $\mathbf{P}_{oo}[k]$ represents the covariance of the observable state estimation error, $\mathbf{P}_{\bar{o}\bar{o}}[k]$ represents that of the unobservable state estimation error, and $\mathbf{P}_{\bar{o}o}[k]$ represents that of the unobservable and observable state estimation errors. Then, we see that

$$\tilde{\mathbf{P}}^-[k]\tilde{\mathbf{C}}^\top = \tilde{\mathbf{A}}\tilde{\mathbf{P}}^-[k-1]\tilde{\mathbf{A}}^\top\tilde{\mathbf{C}}^\top + \tilde{\mathbf{Q}}\tilde{\mathbf{C}}^\top$$

can be represented as

$$\begin{bmatrix} \mathbf{P}_{oo}^-[k] \\ \mathbf{P}_{\bar{o}\bar{o}}^-[k] \end{bmatrix} \mathbf{C}_o^\top = \left(\tilde{\mathbf{A}} \begin{bmatrix} \mathbf{P}_{oo}[k-1] \\ \mathbf{P}_{\bar{o}\bar{o}}[k-1] \end{bmatrix} \mathbf{A}_o^\top + \begin{bmatrix} \mathbf{Q}_o \\ \mathbf{Q}_{\bar{o}} \end{bmatrix} \right) \mathbf{C}_o^\top,$$

where the process noise covariances are defined as

$$\mathbf{Q}_o := (I_2 \otimes V)\mathbf{Q}(I_2 \otimes V)^\top, \quad \mathbf{Q}_{\bar{o}} := \overline{\mathbf{U}}\mathbf{Q}(I_2 \otimes V)^\top.$$

This means that the update equation of $\tilde{P}^- [k]$ is independent of $P_{oo}^- [k]$ and $P_{o\bar{o}} [k]$, and it is given as

$$\begin{bmatrix} P_{oo}^- [k] \\ P_{o\bar{o}}^- [k] \end{bmatrix} = \begin{bmatrix} \mathbf{A}_o & 0 \\ \bar{\mathbf{U}}\mathbf{A}\mathbf{U} & A \end{bmatrix} \begin{bmatrix} P_{oo}^- [k-1] \\ P_{o\bar{o}}^- [k-1] \end{bmatrix} \mathbf{A}_o^\top + \begin{bmatrix} \mathbf{Q}_o \\ \mathbf{Q}_{\bar{o}} \end{bmatrix}.$$

Similarly, the Kalman gain

$$\tilde{\mathbf{H}} [k] = \begin{bmatrix} \mathbf{H}_o [k] \\ H_{\bar{o}} [k] \end{bmatrix}$$

is also independent of them because

$$\begin{bmatrix} \mathbf{H}_o [k] \\ H_{\bar{o}} [k] \end{bmatrix} = \begin{bmatrix} P_{oo}^- [k] \\ P_{o\bar{o}}^- [k] \end{bmatrix} \mathbf{C}_o^\top (\mathbf{C}_o P_{oo}^- [k] \mathbf{C}_o^\top + \mathbf{R})^{-1}.$$

Finally, considering the symmetry of the error covariances, we have the update equations of $P_{oo} [k]$ and $P_{o\bar{o}} [k]$ as

$$\begin{bmatrix} P_{oo} [k] \\ P_{o\bar{o}} [k] \end{bmatrix} = \begin{bmatrix} (I_{2(N-1)} - \mathbf{H}_o [k] \mathbf{C}_o) P_{oo}^- [k] \\ P_{o\bar{o}}^- [k] (I_{2(N-1)} - \mathbf{C}_o^\top \mathbf{H}_o^\top [k]) \end{bmatrix}.$$

Note that $P_{o\bar{o}}$, which is the cause of the indeterminate operations as it diverges over time in the standard Kalman filtering algorithm, is removed from the update equations. In summary, the following Kalman filtering algorithm without indeterminate operations is obtained.

Lemma 1 The Kalman filtering algorithm in (13) and its determinate version given as

$$\left\{ \begin{array}{l} \begin{bmatrix} \hat{\xi}_o^- [k] \\ \hat{\xi}_{\bar{o}}^- [k] \end{bmatrix} = \begin{bmatrix} \mathbf{A}_o & 0 \\ \bar{\mathbf{U}}\mathbf{A}\mathbf{U} & A \end{bmatrix} \begin{bmatrix} \hat{\xi}_o [k-1] \\ \hat{\xi}_{\bar{o}} [k-1] \end{bmatrix} + \begin{bmatrix} \mathbf{B}_o V \\ \bar{\mathbf{U}}\mathbf{B} \end{bmatrix} u[k-1] \\ \begin{bmatrix} P_{oo}^- [k] \\ P_{o\bar{o}}^- [k] \end{bmatrix} = \begin{bmatrix} \mathbf{A}_o & 0 \\ \bar{\mathbf{U}}\mathbf{A}\mathbf{U} & A \end{bmatrix} \begin{bmatrix} P_{oo}^- [k-1] \\ P_{o\bar{o}}^- [k-1] \end{bmatrix} \mathbf{A}_o^\top + \begin{bmatrix} \mathbf{Q}_o \\ \mathbf{Q}_{\bar{o}} \end{bmatrix} \\ \begin{bmatrix} \mathbf{H}_o [k] \\ H_{\bar{o}} [k] \end{bmatrix} = \begin{bmatrix} P_{oo}^- [k] \\ P_{o\bar{o}}^- [k] \end{bmatrix} \mathbf{C}_o^\top (\mathbf{C}_o P_{oo}^- [k] \mathbf{C}_o^\top + \mathbf{R})^{-1} \\ \begin{bmatrix} P_{oo} [k] \\ P_{o\bar{o}} [k] \end{bmatrix} = \begin{bmatrix} (I_{2(N-1)} - \mathbf{H}_o [k] \mathbf{C}_o) P_{oo}^- [k] \\ P_{o\bar{o}}^- [k] (I_{2(N-1)} - \mathbf{C}_o^\top \mathbf{H}_o^\top [k]) \end{bmatrix} \\ \begin{bmatrix} \hat{\xi}_o [k] \\ \hat{\xi}_{\bar{o}} [k] \end{bmatrix} = \begin{bmatrix} \hat{\xi}_o^- [k] \\ \hat{\xi}_{\bar{o}}^- [k] \end{bmatrix} + \begin{bmatrix} \mathbf{H}_o [k] \\ H_{\bar{o}} [k] \end{bmatrix} (y[k] - \mathbf{C}_o \hat{\xi}_o^- [k]) \end{array} \right. \quad (22)$$

are equivalent such that

$$\hat{x}[k] = \mathbf{U} \hat{\xi}_o [k] + (I_2 \otimes \mathbf{1}_N) \hat{\xi}_{\bar{o}} [k], \quad k \in \mathbb{Z}$$

for any basis parameter \mathbf{W} , or equivalently $\bar{\mathbf{W}}$.

Lemma 1 shows that indeterminate operations involved in the standard Kalman filtering algorithm can be removed in an equivalent way. In fact, the stationary values of the error covariances for the determinate equivalent in (22) can be found, while the error covariances for the original algorithm diverge over time.

It should be emphasized that, even if either $\bar{\mathbf{U}}\mathbf{A}\mathbf{U}$ or $\mathbf{Q}_{\bar{o}}$ is zero, the estimation of the unobservable state $\xi_{\bar{o}} [k]$ is not redundant for minimizing the state estimation error. In general, the estimate $\hat{\xi}_{\bar{o}} [k]$ has a non-zero value because the Kalman gain $H_{\bar{o}} [k]$ is not zero in the unobservable part. The estimation of the the unobservable state will play an important role in generating an optimal time scale.

3.3 Determinate Stationary Kalman Filtering Algorithm

Unlike the original algorithm, the determinate Kalman filtering algorithm converges to a stationary algorithm over time. In time scale generation, the properties of such a stationary algorithm are inherently important because clock state estimation continues over a long period of time. To illustrate, we denote the stationary error covariances by

$$P_{oo}^* := \lim_{k \rightarrow \infty} P_{oo}^- [k], \quad P_{o\bar{o}}^* := \lim_{k \rightarrow \infty} P_{o\bar{o}}^- [k],$$

and the stationary Kalman gains by

$$\mathbf{H}_o^* := \lim_{k \rightarrow \infty} \mathbf{H}_o [k], \quad H_{\bar{o}}^* := \lim_{k \rightarrow \infty} H_{\bar{o}} [k].$$

Then, the stationary algorithm is found as follows.

Theorem 1 For the determinate Kalman filtering algorithm in (22), the stationary error covariances are given as the unique solutions to the algebraic equations

$$\begin{aligned} P_{oo}^* &= \mathbf{Q}_o + \mathbf{A}_o P_{oo}^* \mathbf{S} (P_{oo}^*) \mathbf{A}_o^\top, \\ P_{o\bar{o}}^* &= \mathbf{Q}_{\bar{o}} + (A P_{o\bar{o}}^* + \bar{\mathbf{U}}\mathbf{A}\mathbf{U} P_{o\bar{o}}^*) \mathbf{S} (P_{oo}^*) \mathbf{A}_o^\top \end{aligned} \quad (23)$$

where $\mathbf{S} (P_{oo}^*)$ is defined as

$$\mathbf{S} (P_{oo}^*) := I_{2(N-1)} - \mathbf{C}_o^\top (\mathbf{C}_o P_{oo}^* \mathbf{C}_o^\top + \mathbf{R})^{-1} \mathbf{C}_o P_{oo}^*.$$

Furthermore, the stationary algorithm is given as

$$\left\{ \begin{array}{l} \begin{bmatrix} \hat{\xi}_o^- [k] \\ \hat{\xi}_{\bar{o}}^- [k] \end{bmatrix} = \begin{bmatrix} \mathbf{A}_o & 0 \\ \bar{\mathbf{U}}\mathbf{A}\mathbf{U} & A \end{bmatrix} \begin{bmatrix} \hat{\xi}_o [k-1] \\ \hat{\xi}_{\bar{o}} [k-1] \end{bmatrix} + \begin{bmatrix} \mathbf{B}_o V \\ \bar{\mathbf{U}}\mathbf{B} \end{bmatrix} u[k-1] \\ \begin{bmatrix} \hat{\xi}_o [k] \\ \hat{\xi}_{\bar{o}} [k] \end{bmatrix} = \begin{bmatrix} \hat{\xi}_o^- [k] \\ \hat{\xi}_{\bar{o}}^- [k] \end{bmatrix} + \begin{bmatrix} \mathbf{H}_o^* \\ H_{\bar{o}}^* \end{bmatrix} (y[k] - \mathbf{C}_o \hat{\xi}_o^- [k]) \end{array} \right. \quad (24)$$

where the stationary Kalman gains are given as

$$\begin{aligned} \mathbf{H}_o^* &= P_{oo}^* \mathbf{C}_o^\top (\mathbf{C}_o P_{oo}^* \mathbf{C}_o^\top + \mathbf{R})^{-1} \\ H_{\bar{o}}^* &= P_{o\bar{o}}^* \mathbf{C}_o^\top (\mathbf{C}_o P_{oo}^* \mathbf{C}_o^\top + \mathbf{R})^{-1}. \end{aligned} \quad (25)$$

Proof: By considering the recursive update equations in (22) under the conditions that

$$P_{oo}^- [k] = P_{oo}^- [k+1] = P_{oo}^*, \quad P_{o\bar{o}}^- [k] = P_{o\bar{o}}^- [k+1] = P_{o\bar{o}}^*,$$

we have the algebraic equations for P_{oo}^* and $P_{o\bar{o}}^*$ as in (23). The representation of the stationary Kalman gains in (25) are obtained from their update equations.

Next, we prove that P_{oo}^* and $P_{o\bar{o}}^*$ are uniquely determined. The uniqueness of P_{oo}^* is proven because the Kalman filtering algorithm for the observable part coincides with the standard algorithm. On the other hand, to prove the uniqueness of $P_{o\bar{o}}^*$, we use the fact that

$$(I_{2(N-1)} - \mathbf{H}_o^* \mathbf{C}_o)^\top = (I_{2(N-1)} + \mathbf{C}_o^\top R^{-1} \mathbf{C}_o P_{oo}^*)^{-1}.$$

This is proven based on the fact that

$$\mathbf{S} (P_{oo}^*) = (I_{2(N-1)} + \mathbf{C}_o^\top R^{-1} \mathbf{C}_o P_{oo}^*)^{-1},$$

which is known as the matrix inversion lemma. Then, the equation of $P_{o\bar{o}}^*$ in (23) is written as

$$\begin{aligned} P_{o\bar{o}}^* &= A P_{o\bar{o}}^* (I_{2(N-1)} - \mathbf{H}_o^* \mathbf{C}_o)^\top \mathbf{A}_o^\top \\ &\quad + \underbrace{\mathbf{Q}_{\bar{o}} + \bar{\mathbf{U}}\mathbf{A}\mathbf{U} P_{oo}^* (I_{2(N-1)} - \mathbf{H}_o^* \mathbf{C}_o)^\top \mathbf{A}_o^\top}_{\mathbf{X}}. \end{aligned}$$

Using the vectorization of matrices defined as

$$\text{vec}([x_1 \ \cdots \ x_m]) = [x_1^\top \ \cdots \ x_m^\top]^\top,$$

where x_i is a vector, we have the linear equation

$$\text{vec}(P_{oo}^*) = \{A_o(I_{2(N-1)} - H_o^* C_o) \otimes A\} \text{vec}(P_{oo}^*) + \text{vec}(X),$$

which means that P_{oo}^* is uniquely determined if

$$Y := I_{4(N-1)} - \{A_o(I_{2(N-1)} - H_o^* C_o) \otimes A\}$$

is nonsingular. Because H_o^* is the stationary Kalman gain for the observable part, we see that

$$\Lambda(A_o(I_{2(N-1)} - H_o^* C_o)) \subseteq \mathbb{D}.$$

Note that the eigenvalues of A are one. Thus, we have

$$\Lambda(A_o(I_{2(N-1)} - H_o^* C_o) \otimes A) \subseteq \mathbb{D}.$$

This proves that Y is nonsingular. \square

The stationary Kalman filtering algorithm in Theorem 1 does not contain indeterminate operations, nor does it require recursive computation of error covariances. This is a solution to **Q1**. We remark that there is no need to specify the initial error covariances, which also avoids unexpected behavior due to inappropriate initial values in practice. Furthermore, H_o^* can be computed as the standard Kalman gain for the observable state dynamics, while H_o^* can easily be computed from H_o^* without solving a linear matrix equation. This will be shown later.

4 EXPLICIT ENSEMBLE MEAN SYNCHRONIZATION

4.1 General Framework

4.1.1 Specific Choice of Basis Parameter

In the rest of this paper, we consider the stationary Kalman filtering algorithm in (24), because the transient behavior of state estimation is not essential for time scale generation. The main idea is to choose the basis parameter as

$$\overline{W} = I_2 \otimes q^\top. \quad (26)$$

Without loss of generality, we can assume that

$$q^\top \mathbf{1}_N = 1. \quad (27)$$

This is equivalent to selecting

$$W = I_2 \otimes V^+$$

where $V^+ \in \mathbb{R}^{N \times (N-1)}$ is the generalized inverse of V associated with the weight vector q . In particular, using a column full rank matrix $W \in \mathbb{R}^{N \times (N-1)}$ such that

$$q^\top W = 0,$$

we can represent the generalized inverse as

$$V^+ := W(VW)^{-1}.$$

We can easily verify that

$$VV^+ = I_{N-1}, \quad q^\top V^+ = 0. \quad (28)$$

Furthermore, we see that

$$W = U, \quad \overline{W} = \overline{U}.$$

In this parameter choice, the basis expansion is found as

$$x[k] = (I_2 \otimes V^+) \xi_o[k] + (I_2 \otimes \mathbf{1}_N) \xi_{\bar{o}}[k]. \quad (29)$$

Therefore, we can see from (27) and (28) that

$$\xi_{\bar{o}}[k] = (I_2 \otimes q^\top) x[k]$$

represents the unobservable state that corresponds to the weighted average, or explicit ensemble mean, of clocks. On the other hand, the observable state

$$\xi_o[k] = (I_2 \otimes V) x[k]$$

represents the synchronization error from the ensemble mean. Therefore, the control effort to keep the magnitude of the observable state small implies synchronizing the clock states with their ensemble mean, implying that ‘‘explicit’’ ensemble mean synchronization can be achieved.

In this basis parameter choice, we can verify that the observable state dynamics

$$\begin{cases} \xi_o[k+1] = A_o \xi_o[k] + (I_2 \otimes V) v[k] + B_o \omega_o[k] \\ y[k] = C_o \xi_o[k] + w[k] \end{cases} \quad (30a)$$

does not affect the unobservable state dynamics

$$\xi_{\bar{o}}[k+1] = A \xi_{\bar{o}}[k] + (I_2 \otimes q^\top) v[k] + B \omega_{\bar{o}}[k] \quad (30b)$$

where the control input is expanded as

$$u[k] = V^+ \omega_o[k] + \mathbf{1}_N \omega_{\bar{o}}[k]. \quad (30c)$$

Note that $\omega_o[k]$ is the control input to achieve clock synchronization while $\omega_{\bar{o}}[k]$ is the control input to regulate synchronization destination.

4.1.2 Ensemble Mean Synchronization Algorithm

In the following, we analyze the stochastic characteristics of the ensemble mean synchronization algorithm. Because both process noise and measurement noise are assumed to be white and Gaussian, and the system of difference equations is linear, all time sequences of stochastic variables are Gaussian processes.

We consider the specific algorithm to achieve explicit ensemble mean synchronization. The basic strategy is to combine state estimation by the Kalman filtering algorithm with state feedback control. In particular, we apply

$$\begin{cases} \hat{\xi}_o^-[k+1] = A_o \hat{\xi}_o^-[k] + B_o \omega_o[k] + A_o H_o^* (y[k] - C_o \hat{\xi}_o^-[k]) \\ \omega_o[k] = -F_o \hat{\xi}_o^-[k] \end{cases} \quad (31a)$$

for clock synchronization, and

$$\begin{cases} \hat{\xi}_{\bar{o}}^-[k+1] = A \hat{\xi}_{\bar{o}}^-[k] + B \omega_{\bar{o}}[k] + A H_{\bar{o}}^* (y[k] - C_o \hat{\xi}_{\bar{o}}^-[k]) \\ \omega_{\bar{o}}[k] = -F_{\bar{o}}[k] \hat{\xi}_{\bar{o}}^-[k] \end{cases} \quad (31b)$$

for the regulation of synchronization destination. The state estimation part is identical to the determinate Kalman filtering algorithm in (24) with the basis parameter in (26). The feedback gain F_o for the observable part is chosen such that

$$\Lambda(A_o - B_o F_o) \subseteq \mathbb{D}, \quad (32)$$

which is equivalent to the condition that the observable state, or its estimate, is stabilized in the sense of

$$\{\xi_o[k]\}_{k \in \mathbb{Z}} \in \mathcal{G} \iff \{\hat{\xi}_o^-[k]\}_{k \in \mathbb{Z}} \in \mathcal{G}. \quad (33)$$

the equivalence of which follows from

$$\{\xi_o[k] - \hat{\xi}_o^-[k]\}_{k \in \mathbb{Z}} \in \mathcal{G}$$

by the Kalman filtering. On the other hand, the feedback gain $F_o[k]$ for the unobservable part will be specified later.

To analyze the synchronization destination, we consider the free-running ensemble mean dynamics

$$\Pi(q) : \begin{cases} r[k+1] = Ar[k] + (I_2 \otimes q^T)v[k] \\ z[k] = Cr[k]. \end{cases} \quad (34)$$

The synchronization error centered on this synchronization destination is defined as

$$\delta[k] := x[k] - (I_2 \otimes \mathbf{1}_N)r[k]. \quad (35)$$

Then, clock synchronization can be achieved as follows.

Theorem 2 For the clock ensemble model in (10), consider the observable canonical decomposition in (30). Suppose that the feedback gain $F_o[k]$ is zero. Then, the synchronization control algorithm in (31) achieves

$$\{\delta[k]\}_{k \in \mathbb{Z}} \in \mathcal{G} \quad (36)$$

for the free-running ensemble mean dynamics $\Pi(q)$ in (34) if and only if the feedback gain F_o is given as in (32).

Proof: Because $F_o[k]$ is supposed to be zero, the control input $\omega_o[k]$ is zero for the unobservable state dynamics in (30b). Therefore, the dynamics of $\Pi(q)$ in (34) is identical to that of (30b). From the relationship in (29), we see that

$$\delta[k] = (I_2 \otimes V^+) \xi_o[k].$$

Therefore, (32), which is equivalent to (33), implies (36). On the other hand, we have

$$(I_2 \otimes V)\delta[k] = \xi_o[k].$$

Therefore, (36) implies (32). \square

Theorem 2 states that all clocks synchronize with the free-running ensemble mean dynamics $\Pi(q)$ in (34) if and only if the observable state dynamics is stabilized. Note that a desirable feedback gain F_o such that (32) holds can be easily found by a standard technique [13], because the observable state dynamics in (30a) is both controllable and observable. This is a solution to **Q2**.

4.1.3 Application to Clock Steering

The synchronization control algorithm in (31) can also be used as the steering of clocks to a reference clock. We discuss this in more detail as follows. Let us suppose that the N th clock is used as a reference clock to synchronize other clocks. We choose the weight vector as

$$q^T = [0 \ \cdots \ 0 \ 1].$$

Then, the free-running ensemble mean dynamics becomes

$$\Pi(q) : \begin{cases} r[k+1] = Ar[k] + v_N[k] \\ z[k] = Cr[k] \end{cases}$$

where $v_N[k]$ denotes the process noise of the N th clock. This means that the synchronization destination is set to the N th

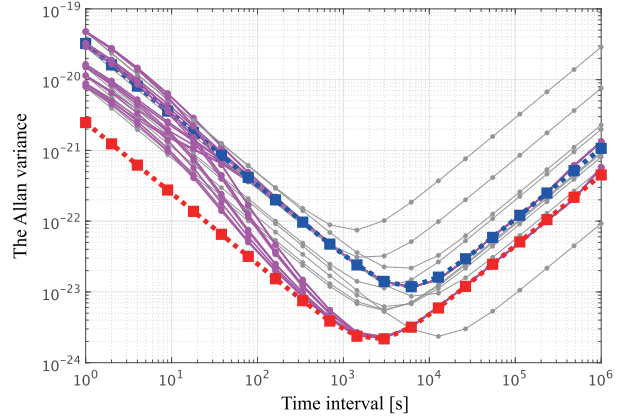


Fig. 3. The Allan variances. The black lines are the analytical Allan variances of the free-running clocks. The blue line is the analytical Allan variances of the free-running reference clock. The red line is the analytical Allan variance of the average of all free-running clocks. The purple lines are the statistical Allan variances of the controlled clocks.

clock being free-running. In fact, the control input $u_N[k]$ to the N th clock is always zero because

$$u_N[k] = q^T u[k] = q^T V^+ \omega_o[k] = 0,$$

where the last equality is proven by (28). All other clocks are synchronized to the reference clock.

For reference, we show the result when this clock steering is applied to the clock ensemble used in Section 2.4.2. We choose the feedback gain in the observable part as

$$F_o = \begin{bmatrix} 0.1 & 1 \\ \tau & 1 \end{bmatrix} \otimes I_9, \quad (37)$$

which satisfies (32). The resulting Allan variance plots are shown in Fig. 3. The black lines correspond to the free-running clocks, which are the same as those in Fig. 1. The blue line correspond to the free-running N th clock. The purple lines correspond to the controlled clocks, i.e., the statistical Allan variance $\mathcal{L}\{h[k]\}_{k \in \mathbb{T}}$ where $h[k]$ denotes the clock reading deviation of the controlled clock ensemble in (10). We can see that all other clocks are synchronized to the reference clock as expected.

We also show in Fig. 3 the result when we choose

$$q = \frac{1}{10} \mathbf{1}_{10},$$

which means that all clocks are synchronized to the simple average. The red line correspond to the average of all free-running clocks. Obviously, the statistical Allan variances of the controlled clocks in this case are generally better than synchronizing to a single clock. However, the generated time scale is not good in the long term.

4.2 Least Allan Variance Synchronization Destination

4.2.1 Optimal Weight Vector for Least Allan Variance

We aim at finding an optimal weight vector that minimizes the Allan variance of the free-running ensemble mean dynamics $\Pi(q)$ in (34). We denote the Allan variance as

$$\sigma_A^2(\tau; \Pi(q)) := \mathbb{E} \left[\frac{(\Delta_1^+ z[k])^2}{2\tau^2} \right], \quad (38)$$

where $\Pi(q)$ should be considered as an implicit function of the sampling interval τ . Then, the optimal weight vector q that gives the least Allan variance is found as follows.

Lemma 2 Consider the free-running ensemble mean dynamics $\Pi(q)$ in (34). Define

$$\Gamma(\tau) := \tau \Sigma_1 + \frac{\tau^3}{3} \Sigma_2. \quad (39)$$

Then, the Allan variance in (38) is given as

$$\sigma_A^2(\tau; \Pi(q)) = \frac{q^\top \Gamma(\tau) q}{\tau^2}. \quad (40)$$

Furthermore, the optimal weight vector

$$q_A(\tau) := \arg \min_q \sigma_A^2(\tau; \Pi(q)) \quad \text{s.t.} \quad q^\top \mathbf{1}_N = 1,$$

which minimizes the Allan variance, is given as

$$q_A(\tau) = \frac{\Gamma^{-1}(\tau) \mathbf{1}_N}{\mathbf{1}_N^\top \Gamma^{-1}(\tau) \mathbf{1}_N}. \quad (41)$$

Proof: By standard calculation, we have

$$\Delta_1^2 z[k] = \underbrace{\begin{bmatrix} C(A - 2I_2) & C \end{bmatrix}}_G \begin{bmatrix} (I_2 \otimes q^\top) v[k] \\ (I_2 \otimes q^\top) v[k+1] \end{bmatrix},$$

where we have used the fact that

$$A^2 - 2A + I_2 = 0.$$

Therefore, the Allan variance can be written as

$$\sigma_A^2(\tau; \Pi(q)) = \frac{1}{2\tau^2} G \left\{ I_2 \otimes \left[(I_2 \otimes q^\top) \mathbf{Q} (I_2 \otimes q) \right] \right\} G^\top,$$

which leads to (40). Furthermore, by the Lagrange multiplier method, the weight vector q that minimizes the Allan variance subject to (27) is found as the solution to

$$\Gamma(\tau)q - \lambda \mathbf{1}_N = 0, \quad q^\top \mathbf{1}_N = 1.$$

Thus, the minimizer is obtained as $q_A(\tau)$ in (41). \square

Lemma 2 gives the optimal weight vector that minimizes the Allan variance of the free-running unobservable state dynamics. In particular, to generate a time scale with better short term stability, it is reasonable to choose

$$q_0 := \lim_{\tau \rightarrow 0} q_A(\tau) = \frac{\Sigma_1^{-1} \mathbf{1}_N}{\mathbf{1}_N^\top \Sigma_1^{-1} \mathbf{1}_N}, \quad (42)$$

which gives the ensemble mean weighted by the inverse ratio of the white frequency noise variances. On the other hand, to generate a time scale with better long term stability, it is reasonable to choose

$$q_\infty := \lim_{\tau \rightarrow \infty} q_A(\tau) = \frac{\Sigma_2^{-1} \mathbf{1}_N}{\mathbf{1}_N^\top \Sigma_2^{-1} \mathbf{1}_N}, \quad (43)$$

which gives the ensemble mean weighted by the inverse ratio of the random walk frequency noise variances.

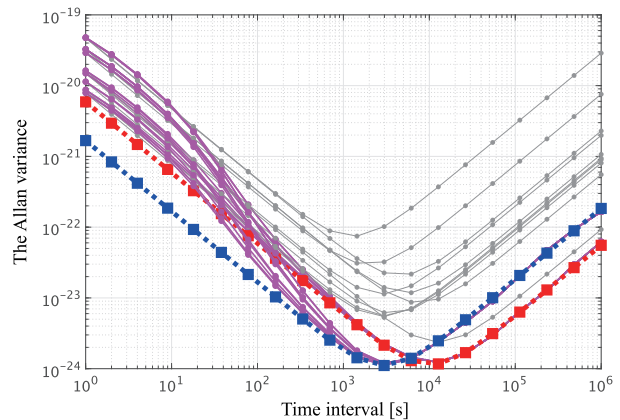


Fig. 4. The Allan variances. The black lines are the analytical Allan variance of the free-running clocks. The blue line is the analytical Allan variance of the best reference time scale in short term. The red line is that in long term. The purple lines are the statistical Allan variance of the controlled clocks.

4.2.2 Need to Balance Short and Long Term Stability

We remark that, unless Σ_1 is a constant multiple of Σ_2 , the weight vector q_0 for better short term frequency stability is not equal to q_∞ for better long term stability. Therefore, it is generally not possible to achieve both short and long term stability as long as the feedback gain $F_o[k]$ is zero.

As an illustration, using the same clock ensemble as in Sections 2.4.2 and 4.1.3, we show in Fig. 4 the results when we choose q_0 and q_∞ . The blue and red lines correspond to the analytical Allan variances $\sigma_A^2(\tau; \Pi(q_0))$ and $\sigma_A^2(\tau; \Pi(q_\infty))$ in (40), respectively. The purple lines correspond to the statistical Allan variances $\mathcal{L}\{h[k]\}_{k \in \mathbb{T}}$ of the controlled clocks. This observation motivates us to achieve a better balance between short and long term stability by properly selecting a non-zero feedback gain $F_o[k]$ for the regulation of the unobservable state dynamics. This will be discussed in the next subsection.

4.3 Balancing Short and Long Term Stability

4.3.1 Kalman Filtering As Explicit Ensemble Mean

To achieve a better balance of short and long term stability, we first prove the following important fact that the determinate Kalman filtering algorithm produces a time scale with the “best” long term stability.

Theorem 3 Consider the stationary version of the determinate Kalman filtering algorithm in (31). Then

$$H_o^* = 0 \quad (44)$$

is satisfied for the unobservable state estimation if and only if the weight vector is chosen as

$$q = q_\infty, \quad (45)$$

where q_∞ is defined as in (43). Furthermore, the stationary error covariances of the unobservable part is given as

$$P_{oo}^* = \begin{bmatrix} 0 & -q_\infty^\top \Sigma_1 V^\top \\ 0 & 0 \end{bmatrix}. \quad (46)$$

Proof: We first prove that (44) implies (45). We see from (25) that, if (44) holds, then

$$P_{\bar{o}o}^* C_o^T = 0,$$

which means that $P_{\bar{o}o}^*$ is structured as

$$P_{\bar{o}o}^* = \begin{bmatrix} 0 & p_1^T \\ 0 & p_2^T \end{bmatrix},$$

where p_i is a vector. Furthermore, we see from (23) that

$$P_{\bar{o}o}^* = Q_{\bar{o}} + AP_{\bar{o}o}^* A_o^T,$$

which can be rewritten as

$$\begin{bmatrix} q^T \Gamma(\tau) V^T & \frac{\tau^2}{2} q^T \Sigma_2 V^T \\ \frac{\tau^2}{2} q^T \Sigma_2 V^T & \tau q^T \Sigma_2 V^T \end{bmatrix} = \begin{bmatrix} -\tau(p_1^T + \tau p_2^T) & -\tau p_2^T \\ -\tau p_2^T & 0 \end{bmatrix}.$$

Thus, the equality of the (2,2)-block leads to (45).

Conversely, if (45) holds, then we have

$$Q_{\bar{o}} = \begin{bmatrix} \tau q_\infty^T \Sigma_1 V^T & 0 \\ 0 & 0 \end{bmatrix}.$$

By substitution, it can be verified that (46) is the solution to the algebraic equation

$$P_{\bar{o}o}^* = Q_{\bar{o}} + AP_{\bar{o}o}^* (I_{2(N-1)} - H_o^* C_o)^T A_o^T$$

for any H_o^* . Therefore, we obtain

$$H_o^* = P_{\bar{o}o}^* C_o^T (C_o P_{\bar{o}o}^* C_o^T + R)^{-1} = 0.$$

This proves the claim. \square

Theorem 3 shows that the time scale generation based on the Kalman filtering can be understood as a special case of the explicit ensemble mean synchronization. More specifically, if we choose the weight vector q in (45), then the synchronization control algorithm in (31) with $F_{\bar{o}}[k]$ equal to zero can achieve the best long term stability. This conversely implies that the time scale generation based on the Kalman filtering is generally not optimal in terms of short term stability. This is a solution to Q3.

4.3.2 Kalman Gain for Unobservable State Estimation

As an application of Theorem 3, we can find a simple algorithm to compute the Kalman gain $H_{\bar{o}}^*$ for the unobservable state estimation in a general choice of the basis. For explanation, we represent the basis expansion associated with the weight vector q_∞ as

$$x[k] = (I_2 \otimes V_\infty^+) \zeta_o[k] + (I_2 \otimes \mathbf{1}_N) \zeta_{\bar{o}}[k] \quad (47)$$

where V_∞^+ denotes the generalized inverse of V associated with q_∞ . In particular, V_∞^+ can be defined as

$$V_\infty^+ := W_\infty (V W_\infty)^{-1}$$

where W_∞ is a column full rank matrix such that

$$q_\infty^T W_\infty = 0.$$

Then, we can see from (29) that

$$\begin{bmatrix} \xi_o[k] \\ \xi_{\bar{o}}[k] \end{bmatrix} = \begin{bmatrix} I_{2(N-1)} & 0 \\ I_2 \otimes q^T V_\infty^+ & I_2 \end{bmatrix} \begin{bmatrix} \zeta_o[k] \\ \zeta_{\bar{o}}[k] \end{bmatrix}. \quad (48)$$

Considering the Kalman gains in these two bases, we have

$$\begin{bmatrix} H_o^* \\ H_{\bar{o}}^* \end{bmatrix} = \begin{bmatrix} I_{2(N-1)} & 0 \\ I_2 \otimes q^T V_\infty^+ & I_2 \end{bmatrix} \begin{bmatrix} H_o^* \\ 0 \end{bmatrix}.$$

Therefore, $H_{\bar{o}}^*$ can be computed as

$$H_{\bar{o}}^* = (I_2 \otimes q^T V_\infty^+) H_o^*,$$

where H_o^* can be computed as the standard Kalman gain for the observable state dynamics. In a similar way, the error covariance $P_{\bar{o}o}^*$ in a general basis can be found as

$$P_{\bar{o}o}^* = (I_2 \otimes q^T V_\infty^+) P_{oo}^* + \begin{bmatrix} 0 & -q_\infty^T \Sigma_1 V^T \\ 0 & 0 \end{bmatrix}.$$

4.3.3 Correction To Optimize Long Term Stability

As shown in (21), the Kalman filtering algorithm is independent of the particular basis choice. Thus, the estimation of the unobservable state can be used as a correction to improve long term stability. In particular, using

$$m\mathbb{Z} := \{mk : k \in \mathbb{Z}\},$$

we apply a corrective input with a longer period as

$$F_{\bar{o}}[k] = \begin{cases} K_{\bar{o}}, & k \in m\mathbb{Z} \\ 0, & \text{otherwise.} \end{cases} \quad (49a)$$

This means that the corrective input $\omega_{\bar{o}}[k]$ is applied every m steps. The resulting intermitted dynamics of the unobservable state estimation in (31b) is

$$\hat{\xi}_o^-[k+m] = A^m \hat{\xi}_o^-[k] + \eta[k] + A^{m-1} B \omega_{\bar{o}}[k], \quad k \in m\mathbb{Z},$$

where the sum of innovations is denoted as

$$\eta[k] := \sum_{i=0}^{m-1} A^{m-1-i} H_{\bar{o}}^* (y[k+i] - C_o \hat{\xi}_o^-[k+i]),$$

which is known to be a white Gaussian process. To stabilize the unobservable state estimation dynamics, the feedback gain $K_{\bar{o}}$ is chosen such that

$$\Lambda(A^m - A^{m-1} B K_{\bar{o}}) \subseteq \mathbb{D}, \quad (49b)$$

which is equivalent to

$$\{\hat{\xi}_{\bar{o}}^-[k]\}_{k \in m\mathbb{Z}} \in \mathcal{G}.$$

We can see that

$$A^m = \begin{bmatrix} 1 & m\tau \\ 0 & 1 \end{bmatrix}, \quad A^{m-1} B = \begin{bmatrix} m\tau \\ 1 \end{bmatrix},$$

which correspond to the system matrices obtained with the sampling interval $m\tau$.

Because of the intermittency of the corrective input to the unobservable state dynamics, it is clear that

$$\xi_{\bar{o}}[k+1] = A \xi_{\bar{o}}[k] + (I_2 \otimes q^T) v[k], \quad k \notin m\mathbb{Z}.$$

This means that, if q_0 in (42) is chosen as the weight vector, then during the period when no corrective input is given, the unobservable state dynamics follows the dynamics of $\Pi(q_0)$, which has the best short term stability.

On the other hand, owing to the corrective input, the unobservable state dynamics in the long term follows the dynamics of $\Pi(q_\infty)$, which has the best long term stability. This fact is proven as follows.

Theorem 4 For the clock ensemble model in (10), consider the observable canonical decomposition in (30). Suppose that the weight vector q is not equal to q_∞ in (43). Then, the synchronization control algorithm in (31) achieves

$$\{\delta[k]\}_{k \in m\mathbb{Z}} \in \mathcal{G} \quad (50)$$

for the free-running ensemble mean dynamics $\Pi(q_\infty)$ in (34) if and only if the feedback gains F_o and $F_o[k]$ are given as in (32) and (49), respectively.

Proof: Consider the basis expansion in (47) associated with the weight vector q_∞ . Correspondingly, we consider the expansion of the control input as

$$u[k] = V_\infty^+ \nu_o[k] + \mathbf{1}_N \nu_{\bar{o}}[k].$$

Then, $\delta[k]$ in (35) can be represented as

$$\delta[k] = (I_2 \otimes V_\infty^+) \zeta_o[k] + (I_2 \otimes \mathbf{1}_N) (\zeta_{\bar{o}}[k] - r[k]).$$

Because $\zeta_{\bar{o}}[k]$ and $r[k]$ follow the dynamics of

$$\begin{aligned} \zeta_{\bar{o}}[k+1] &= A \zeta_{\bar{o}}[k] + (I_2 \otimes q_\infty^T) v[k] + B \nu_{\bar{o}}[k], \\ r[k+1] &= A r[k] + (I_2 \otimes q_\infty^T) v[k], \end{aligned}$$

we can see that the difference state

$$\hat{\zeta}_{\bar{o}}^-[k] := \zeta_{\bar{o}}[k] - r[k]$$

follows the dynamics of

$$\hat{\zeta}_{\bar{o}}^-[k+1] = A \hat{\zeta}_{\bar{o}}^-[k] + B \nu_{\bar{o}}[k].$$

This corresponds to the Kalman filtering algorithm of the unobservable state $\zeta_{\bar{o}}[k]$ because the Kalman gain of the unobservable part must be zero, as shown in Theorem 3. Therefore, the whole Kalman filtering algorithm in this basis choice is found as

$$\begin{cases} \zeta_o[k+1] = \mathbf{A}_o \zeta_o[k] + (I_2 \otimes V) v[k] + \mathbf{B}_o \nu_o[k] \\ \hat{\zeta}_{\bar{o}}^-[k+1] = \mathbf{A}_o \hat{\zeta}_{\bar{o}}^-[k] + \mathbf{B}_o \nu_o[k] + \mathbf{A}_o \mathbf{H}_o^* (y[k] - \mathbf{C}_o \hat{\zeta}_{\bar{o}}^-[k]) \\ \hat{\zeta}_{\bar{o}}^-[k+1] = A \hat{\zeta}_{\bar{o}}^-[k] + B \nu_{\bar{o}}[k] \\ y[k] = \mathbf{C}_o \zeta_o[k] + w[k]. \end{cases}$$

Note that this system of difference equations is equivalent to the system of (30) and (31). In particular, the system states and their estimates satisfy the one-to-one relation as in (48). In the same way, the control inputs satisfy

$$\begin{bmatrix} \nu_o[k] \\ \nu_{\bar{o}}[k] \end{bmatrix} = \begin{bmatrix} I_{N-1} & 0 \\ q_\infty^T V^+ & 1 \end{bmatrix} \begin{bmatrix} \omega_o[k] \\ \omega_{\bar{o}}[k] \end{bmatrix}.$$

Note that $q_\infty^T V^+$ is not zero because q is not equal to q_∞ . Therefore, the entire system of difference equations is internally stabilized at every m steps if and only if the feedback gains F_o and $F_o[k]$ are given as in (32) and (49), respectively. This proves the claim. \square

Theorem 4 shows that long term stability is optimized by feeding back the estimate of the unobservable state, regardless of the choice of the weight vector q . To achieve a better balance between short and long term stability, we propose to choose the weight vector as q_0 so that the unobservable state dynamics follows $\Pi(q_0)$ in the short term, while following $\Pi(q_\infty)$ in the long term. This is a solution to **Q4**.

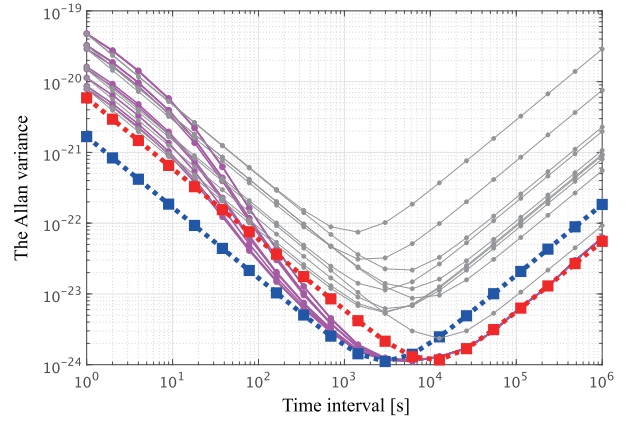


Fig. 5. The Allan variances. The black lines are the analytical Allan variance of the free-running clocks. The blue line is the analytical Allan variance of the best reference time scale in short term. The red line is the analytical Allan variance of the best reference time scale in long term. The purple lines are the statistical of the controlled clocks.

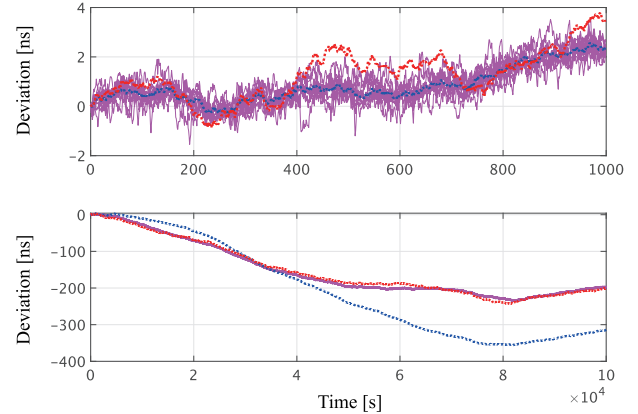


Fig. 6. Time sequences of clock reading deviations. The upper subfigure shows a short period of time, while the lower shows a long period of time. The blue line is the best reference time scale in short term. The red line is the best reference time scale in long term. The purple lines are the controlled clocks.

4.3.4 Demonstration of Optimal Time Scale Generation

Using the same clock ensemble as in Sections 2.4.2, 4.1.3, and 4.2.2, we show the result when we optimize both short and long term stability. With the sampling interval of 1 [s], we consider applying the corrective input every 200 [s], i.e., we take m as 200. We choose the feedback gain for the unobservable state dynamics as

$$K_{\bar{o}} = \begin{bmatrix} \frac{0.01}{m\tau} & 1 \end{bmatrix},$$

which satisfies (49b).

The result is shown in Fig. 5. The blue and red lines correspond to the analytical Allan variances $\sigma_A^2(\tau; \Pi(q_0))$ and $\sigma_A^2(\tau; \Pi(q_\infty))$, respectively. The purple lines correspond to the statistical Allan variances $\mathcal{L}\{h[k]\}_{k \in \mathbb{T}}$ of the controlled clocks. Contrary to Fig. 4, the statistical Allan variances of the controlled clocks are optimized in the long term.

Fig. 5 shows the time sequences $\{h[k]\}_{k \in \mathbb{T}}$ of the controlled clock reading deviations. The upper subfigure shows

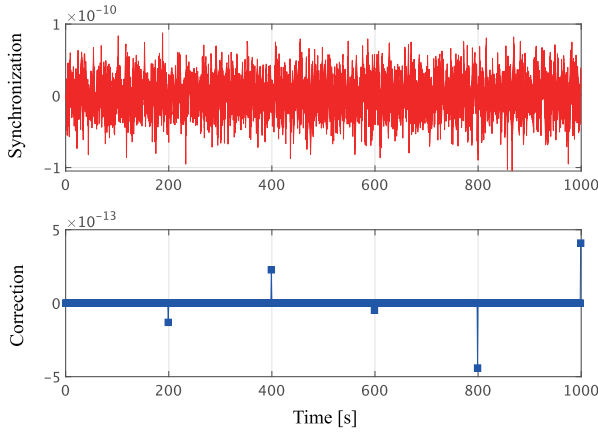


Fig. 7. Input sequences. The upper subfigure shows the control inputs for synchronization, while the lower shows the corrective inputs for the regulation of synchronization destination.

the period of 1,000 [s], while the lower figure shows the period of 100,000 [s]. The blue line is the best reference time scale in short term, i.e., $\{z[k]\}_{k \in \mathbb{T}}$ of $\Pi(q_0)$, while the red line is the best reference time scale in long term, i.e., $\{z[k]\}_{k \in \mathbb{T}}$ of $\Pi(q_\infty)$. The purple lines are the controlled clocks. We can see that the controlled clocks follow the dynamics of $\Pi(q_0)$ in the short term, while they follow the dynamics of $\Pi(q_\infty)$ in the long term, as expected.

Finally, we show the resulting control inputs in Fig. 7. The upper subfigure shows the control input $\{\omega_o[k]\}_{k \in \mathbb{T}}$ for synchronization, while the lower shows the corrective input $\{\omega_\sigma[k]\}_{k \in \mathbb{T}}$ for regulating synchronization destination. By design, the corrective input is given every 200 [s].

5 CONCLUDING REMARKS

In this paper, we have presented a unified framework for atomic time scale generation, called explicit ensemble mean synchronization. By applying an observable canonical decomposition to a standard atomic clock ensemble model, we showed that the system dynamics can be decoupled into an observable part representing the synchronization deviation and an unobservable part capturing the synchronization destination. This decomposition allowed us to reinterpret standard Kalman filtering, commonly used in current time scale generation, as a special case of the proposed framework.

Furthermore, we formulate a control-theoretic algorithm that synchronizes all clocks to a specified ensemble mean and balances both short-term and long-term stability of the generated time scale by incorporating feedback control of the synchronization destination. Notably, the proposed framework not only eliminates the indeterminate operations inherent in conventional Kalman filtering, but also provides a systematic method for both clock synchronization and optimal time scale generation. This framework provides a principled basis for robust timekeeping systems that goes beyond conventional approaches in both scope and performance.

ACKNOWLEDGMENT

This work is supported by research and development conducted by the Ministry of Internal Affairs and Communications (MIC) under its "Research and Development for Expansion of Radio Resources (JPJ000254)" program.

REFERENCES

- [1] L. Galleani, G. Signorile, V. Formichella, and I. Sesia, "Generating a real-time time scale making full use of the available frequency standards," *Metrologia*, vol. 57, no. 6, p. 065015, 2020.
- [2] N. Nemitz, T. Gotoh, F. Nakagawa, H. Ito, Y. Hanado, T. Ido, and H. Hachisu, "Absolute frequency of 87sr at 1.8×10^{-16} uncertainty by reference to remote primary frequency standards," *Metrologia*, vol. 58, no. 2, p. 025006, 2021.
- [3] H. S. Lee, T. Y. Kwon, S. E. Park, Y. K. Lee, S.-h. Yang, D.-H. Yu, M.-S. Heo, H. Kim, C. Y. Park, and W.-K. Lee, "Characteristics of a real-time ensemble time scale corrected by the kriss-psfs using a reduced kalman filter (kred) algorithm," *Metrologia*, vol. 60, no. 4, p. 045006, 2023.
- [4] L. Galleani and P. Tavella, "On the use of the kalman filter in timescales," *Metrologia*, vol. 40, no. 3, p. S326, 2003.
- [5] L. Cosart, H. Imlau, and G. Zampetti, "cnprtc—coherent network primary reference time clock: a geographically distributed resilient timescale for telecommunications," *IEEE Communications Magazine*, vol. 61, no. 4, pp. 28–32, 2022.
- [6] E. F. Arias, G. Panfilo, and G. Petit, "Timescales at the bipm," *Metrologia*, vol. 48, no. 4, pp. S145–S153, 2011.
- [7] L. Galleani and P. Tavella, "Time and the Kalman filter," *IEEE Control Systems*, vol. 30, pp. 44–65, 4 2010.
- [8] K. R. B. Jr, "The theory of the GPS composite clock," pp. 223–242, 9 1991. [Online]. Available: <http://www.ion.org/publications/abstract.cfm?jp=p&articleID=4867>
- [9] C. A. Greenhall, "A review of reduced Kalman filters for clock ensembles," *IEEE Transactions on Ultrasonics, Ferroelectrics, and Frequency Control*, vol. 59, pp. 491–496, 3 2012.
- [10] —, "A Kalman filter clock ensemble algorithm that admits measurement noise," *Metrologia*, vol. 43, p. S311, 8 2006.
- [11] L. Galleani, "A tutorial on the two-state model of the atomic clock noise," *Metrologia*, vol. 45, pp. S175–S182, 12 2008.
- [12] R. E. Kalman, "A new approach to linear filtering and prediction problems," *Journal of Basic Engineering*, vol. 82, pp. 35–45, 3 1960.
- [13] F. W. Fairman, *Linear control theory: the state space approach*. John Wiley & Sons, 1998.
- [14] D. Allan, "Statistics of atomic frequency standards," *Proceedings of the IEEE*, vol. 54, pp. 221–230, 1966.
- [15] C. Zucca and P. Tavella, "The clock model and its relationship with the Allan and related variances," *IEEE Transactions on Ultrasonics, Ferroelectrics and Frequency Control*, vol. 52, pp. 289–296, 2 2005.
- [16] T. Ishizaki, T. Ichimura, T. Kawaguchi, Y. Yano, and Y. Hanado, "Higher-order Allan variance for atomic clocks of arbitrary order: mathematical foundation," *Metrologia*, vol. 61, 2 2024.
- [17] D. S. Bernstein, *Matrix mathematics: theory, facts, and formulas*. Princeton University Press, 2009.
- [18] A. C. Antoulas, *Approximation of large-scale dynamical systems*. Society for Industrial and Applied Mathematics, 2005.